



Predicting the severity of Swiss needle cast on Douglas-fir under current and future climate in New Zealand

Michael S. Watt^{a,*}, Jeffrey K. Stone^b, Ian A. Hood^c, David J. Palmer^c

^a Scion, PO Box 29237, Fendalton, Christchurch 8540, New Zealand

^b Department of Botany and Plant Pathology, Oregon State University, Corvallis, OR 97331, USA

^c Scion Forest Biosecurity and Protection, Private Bag 3020, Rotorua 3046, New Zealand

ARTICLE INFO

Article history:

Received 6 August 2010

Received in revised form

20 September 2010

Accepted 20 September 2010

Keywords:

Climate change

Phaeocryptopus gaemannii

Pseudotsuga menziesii

Spatial modelling

ABSTRACT

Phaeocryptopus gaemannii, the causal agent of Swiss needle cast, is widely distributed in plantations of Douglas-fir (*Pseudotsuga menziesii*) throughout New Zealand, causing premature abscission of needles and significant growth losses. Data were collected from 34 sites, selected to span a broad range of environmental conditions within New Zealand, to (i) develop models of infection and foliage retention, F_{ret} , and (ii) from these models predict F_{ret} by region under current and future climates, using the factorial combination of 12 Global Climate Models (GCMs) and three emission scenarios (low, B1; medium, A1B; and high, A2).

Pathogen abundance, as measured by a colonisation index (CI_{norm}), was found to exhibit a significant positive linear relationship ($R^2 = 0.53$; $P < 0.001$) with early winter (June) air temperature, and a marginally significant quadratic relationship ($R^2 = 0.19$, $P < 0.036$) with late spring (November) rainfall that increased to a maximum at 149 mm month⁻¹, before declining. In combination these two variables accounted for 64% of the variation in CI_{norm} among sites. Predicted CI_{norm} was the single variable most strongly correlated with measured F_{ret} . The relationship between predicted CI_{norm} and F_{ret} was described by a significant ($P < 0.001$) negative linear relationship that accounted for 51% of the variation in the data. Addition of further climatic variables did not significantly improve predictive power of this model for F_{ret} .

Under the current climate, spatial predictions of F_{ret} were between 70% and 100% for most of the South Island, and between 40% and 70% for most of the North Island. When projected out to 2040 there was little change in F_{ret} . However, projections out to 2090 showed substantial reductions in F_{ret} that were positively related to the three forecast emission levels. These reductions averaged 6.5%, 10.1%, and 13.7% for the B1, A1B and A2 emission scenarios, respectively. Reductions in F_{ret} were particularly marked within the North Island under the A1B and A2 emission scenarios. Apart from coastal and low lying regions, large areas within the South Island were projected to sustain relatively low levels of disease, and remain suitable for Douglas-fir.

© 2010 Elsevier B.V. All rights reserved.

1. Introduction

Swiss needle cast is a foliage disease caused by the ascomycete *Phaeocryptopus gaemannii* (Rohde) Petrak, which occurs naturally in indigenous *Pseudotsuga menziesii* (Mirb.) Franco (Douglas-fir) forests in western North America. The fungus was initially discovered and described from diseased Douglas-fir plantations in Switzerland in 1925, and soon afterward reported from other locations in Europe (Boyce, 1940). Infection by this fungus frequently results in chlorotic foliage, defoliation and growth reduction. Outbreaks of Swiss needle cast have occurred in both native and plantation grown *P. menziesii* in the Pacific Northwest (Hansen et

al., 2000; Manter et al., 2005; Stone et al., 2008b) and forest plantations in Europe and the United Kingdom (Boyce, 1940; Peace, 1962), the northeastern U.S. (Morton and Patton, 1970), Turkey (Temel et al., 2003), Australia (Marks et al., 1989) and New Zealand (Hood et al., 1990). More recently Swiss needle cast has been recognized as an emerging disease within the native Douglas-fir range in the U.S. Pacific Northwest. In western Oregon growth reductions associated with increasing disease severity have occurred since the mid-1980s and approximately 160,000 ha are currently affected by the disease (Black et al., 2010).

For Swiss needle cast, there is a sound physiological basis that links the abundance of *P. gaemannii* with disease severity. Fruiting bodies (pseudothecia) of *P. gaemannii* physically occlude the stomata of Douglas-fir needles, thereby impairing gas exchange and photosynthesis (Manter et al., 2003). The premature loss of foliage and resulting growth reduction in Douglas-fir are thus directly

* Corresponding author. Tel.: +64 3 364 2949; fax: +64 3 364 2812.

E-mail address: michael.watt@scionresearch.com (M.S. Watt).

related to a decrease in CO₂ assimilation that in turn is directly linked to the abundance of the pathogen (Manter et al., 2003). This relationship has been convincingly demonstrated in both Oregon and New Zealand by using the proportion of occluded stomata as a measure of pathogen abundance to quantify foliage loss (Stone et al., 2007). It should be possible to use this relationship to develop spatial surfaces that describe variation in foliage retention across wide environmental ranges, since there is clear evidence that the abundance of *P. gaemannii* is regulated by climate (Hood, 1982; Manter et al., 2005; Stone et al., 2007). Such predictions of the disease would be of considerable use to forest managers, as foliage retention has been found to be the key determinant of volume loss in Douglas-fir (Maguire et al., 2002).

To achieve this objective it is necessary to quantify and refine the relationship between disease and various climate variables and much has already been achieved. In the Oregon Coast Range ~80% of the spatial variation in pathogen abundance was attributable to winter mean daily temperature and spring cumulative leaf wetness (Manter et al., 2005), with abundance increasing under warm wet conditions (Manter et al., 2005). Strong positive relationships between winter temperature and pathogen abundance, of a very similar form to those noted in Oregon, have also been found in Douglas-fir stands covering a wide environmental range in New Zealand (Stone et al., 2007).

Given the responsiveness of the pathogen to variations in air temperature, climate change is likely to have a marked effect on pathogen distribution, disease severity and host productivity. Pathogens have shorter generation times than trees and so their populations can be expected to respond more rapidly to climate change. Consequently, over the rotation interval of a forest, Swiss needle cast has the potential to cause significant growth reduction in a plantation that may have been only marginally at risk at the time of establishment. The development of models that account for this variation in impact over the course of a crop life is critical for making informed decisions on where to site Douglas-fir plantations under increasingly rapid rates of climate change.

Using measurements collected from young (10–15-year old) Douglas-fir stands selected to represent the full range of environmental conditions for Douglas-fir cultivation in New Zealand, the objectives of this study were to (i) construct models that best describe spatial variation in pathogen abundance and foliage retention (ii) using these models develop spatial predictions of pathogen abundance and foliage retention of Douglas-fir in New Zealand under current climate and (iii) using a comprehensive set of 36 climate change scenarios determine F_{ret} of Douglas-fir for both 2040 and 2090 in New Zealand.

2. Materials and methods

2.1. Sampling sites

Sampling was conducted between October and December of both 2005 and 2007 in Douglas-fir plantations at 34 sites that covered a large number of regions (Fig. 1) and a wide environmental gradient (Table 1). This period spans the southern hemisphere spring and early summer and was timed to coincide with the peak sporulation of *P. gaemannii* immediately following bud burst (Hood and Kershaw, 1975). Selected plantations were 10–15 years old at the time of sampling, to minimize the variation due to changes in canopy conditions with tree age. A total of 16 sites were sampled in 2005 and 32 in 2007, including 14 of those evaluated during the first sampling (Fig. 1).

In order to account for potential host genetic effects, 10 of the 34 sites sampled in both years were chosen as part of a Douglas-fir trial series established throughout the country in 1996 (see Stone

Region

- 1: Auckland
- 2: Bay of Plenty
- 3: Canterbury
- 4: Gisborne
- 5: Hawke's Bay
- 6: Manawatu-Wanganui
- 7: Marlborough
- 8: Nelson
- 9: Northland
- 10: Otago
- 11: Southland
- 12: Taranaki
- 13: Tasman
- 14: Waikato
- 15: Wellington
- 16: West Coast

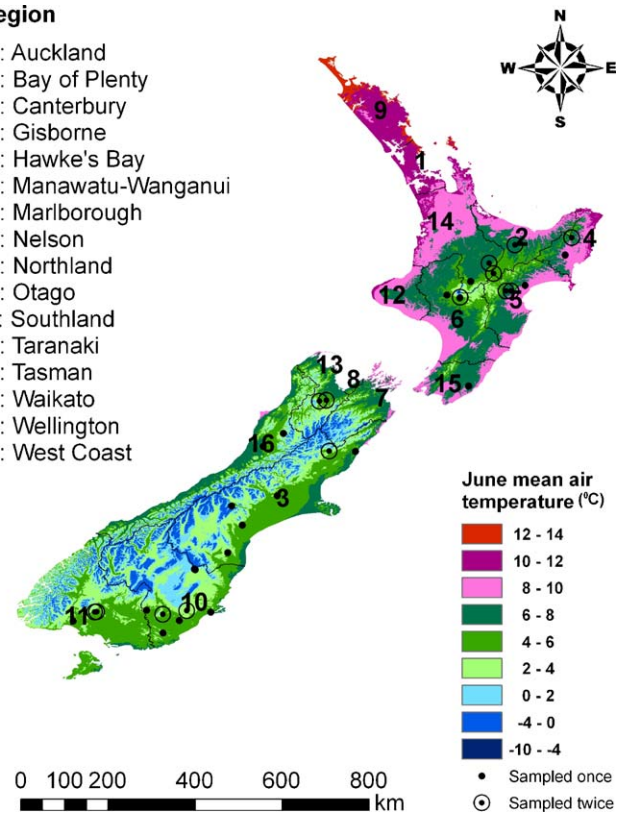


Fig. 1. Map of New Zealand showing the distribution of the study sites, in relation to June mean air temperature. Sites were either sampled once (solid circles) or twice (solid circles, with ring). New Zealand regional boundaries are shown on the map.

et al., 2007 for a detailed description). Three seedlots derived from parent trees grown in New Zealand were selected whose original provenances were: Fort Bragg, California, coastal Oregon and western Washington. These seedlots are widely planted in young (<20-year-old) Douglas-fir plantations in New Zealand and were also represented in 14 of the non-trial sites. At each site, and in each of the three New Zealand seedlots in the progeny and seed source trial stands, 10–15 trees were arbitrarily selected for foliage retention assessments and foliage sampling.

Table 1

Variation in location, climate, foliage retention (F_{ret}) and normalised colonisation index (CI_{norm}) across sites.

| Variable | Mean | Min. | Max. |
|-------------------------------------|-----------------|--------|-------|
| Location | | | |
| Latitude (°) | -42.4 ± 3.0 | -46.3 | -38.1 |
| Longitude (°) | 172.8 ± 3.2 | 167.6 | 177.9 |
| Altitude (m) | 482 ± 221 | 130 | 933 |
| Climate-general | | | |
| Mean av. temp (°C) | 9.7 ± 1.4 | 7.1 | 12.4 |
| Mean min. temp (°C) | 4.9 ± 1.5 | 2.1 | 8.2 |
| Total rain (mm year ⁻¹) | 1341 ± 451 | 672 | 2532 |
| Climate-in analysis | | | |
| Mean June temp. (°C) | 4.9 ± 1.7 | 1.5 | 8.2 |
| Nov. total rain (mm) | 110 ± 45 | 64 | 269 |
| Pathogen and disease | | | |
| CI year 1 needles | 5.3 ± 5.6 | 0.01 | 24.3 |
| CI year 2 needles | 17.2 ± 13.7 | 0.02 | 54.0 |
| CI_{norm} | 0.3 ± 0.3 | 0.0004 | 1 |
| F_{ret} (%) | 78.6 ± 16.9 | 40 | 100 |

Shown are the mean, followed by the standard deviation, and the minimum (Min.) and maximum (Max.) values.

2.2. Foliage retention

Foliage retention was assessed in the field by the same person at all sites in both years. For each tree, two secondary branches subtended at the 4th (basal) node on the primary axis of one 5th whorl primary branch were cut with a pole pruner. Foliage retention was visually estimated by using a 0–9 (0 ≤ 10% of needles attached, 9 ≥ 90% of needles attached) scale for each of the four internodes, aged from one to four years at the time of sampling. Values were summed for all foliage classes ($x=0-36$) and then rescaled as a percentage foliage retention, F_{ret} , for analyses ($F_{\text{ret}} = x/36 \times 100$). A sample of four to six tertiary shoots bearing one and two year old internodes was collected from the same basal secondary branch on each tree and sealed in a labeled polythene bag (one bag per tree). Samples were held at 4 °C until processed in the laboratory within 2 weeks of collection.

2.3. *P. gaeumannii* abundance

Foliage samples were returned to the laboratory where the one- and two-year old internodes were separated, needles removed from branchlets and pooled by age class. A sample of 50 needles for each age class per tree was randomly drawn, needles affixed with the abaxial surface facing upwards to a labeled index card with double sided adhesive tape, and the cards stored frozen (−20 °C) until examined.

To estimate abundance of *P. gaeumannii* each 50-needle sample was examined under a binocular dissecting microscope at 40× to determine the proportion of needles bearing pseudothecia (incidence of infection). The first ten needles on each card with pseudothecia present were then used to determine the proportion of stomata occluded by pseudothecia (pseudothecial density). The needles were examined under a dissecting microscope fitted with a counting grid and the proportion of stomata occluded by pseudothecia in three, 2.6 mm × 0.26 mm segments (base, middle, tip) of each of the ten needles was determined and averaged. A colonisation index (CI) was determined as the product of the percent of needles with visible pseudothecia (incidence, $n=50$) and the average proportion of stomata occluded (pseudothecial density, $n=10$).

2.4. Meteorological data

Meteorological data used in analyses to define current climate were obtained from thin-plate spline surfaces (Hutchinson and Gessler, 1994) fitted to meteorological station data, at a spatial resolution of 100 m (Leathwick and Stephens, 1998). Data used to fit these surfaces cover the period 1951–1980 (New Zealand Meteorological Service, 1983). The average New Zealand air temperature based on 7 long-running climate stations (Salinger, 1981; NIWA, 2010) has increased over the last century by approximately 0.9 °C. Using this rate of change (0.009 °C year^{−1}) we updated these temperature surfaces from the midpoint of measurements used for surface construction (1965) to the mean time at which field measurements were made in this study (2006) by adding 0.369 °C to all temperature values (0.009 °C year^{−1} × (2006–1965)). As no significant trends in precipitation have been noted in New Zealand over the last century (Tait, A., NIWA, personal communication) this surface was left unchanged. For the purposes of this study these surfaces were used to define the “current climate”.

Climate change projections used in this study were derived from the factorial combination of 12 Global Climate Models (GCMs) and the B1 (low), A1B (mid-range) and A2 (high) emission scenarios, that have been fully described, previously (Ministry for the Environment, 2008). The 12 GCMs used in this study are abbreviated to: CNRM, CCCma, CSIRO Mk3, GFDL CM 2.0, GFDL CM 2.1, MIROC32, ECHOG, ECHAM5, MRI, NCAR, UKMO-HadCM3, UKMO-

Table 2

Summary of changes in air temperature and rainfall under the climate change scenarios, in relation to current climate.

| Year | Emission scenario | Temperature change (°C) | | | Rainfall change (%) | | |
|------|-------------------|-------------------------|-------|------|---------------------|-------|------|
| | | Mean | Min. | Max. | Mean | Min. | Max. |
| 2040 | B1 | 0.57 | 0.28 | 0.95 | 2.2 | −9.3 | 11.7 |
| | A1B | 0.73 | 0.31 | 1.13 | −0.3 | 7.5 | 11.6 |
| | A2 | 0.73 | −0.04 | 1.00 | −0.7 | −5.7 | 7.6 |
| 2090 | B1 | 1.25 | 0.48 | 2.20 | 0.1 | −9.7 | 11.5 |
| | A1B | 1.93 | 0.88 | 3.01 | −2.6 | −18.1 | 14.1 |
| | A2 | 2.50 | 1.35 | 3.18 | 1.0 | −17.0 | 14.9 |

Values shown give the mean New Zealand change pooled across the 12 Global Climate Models (GCMs), within each emission scenario. The minimum (Min.) and maximum (Max.) indicate the mean New Zealand change, for the GCMs representing lowest and highest respective mean changes in air temperature and rainfall.

HadGEM1. Temperature and rainfall were statistically downscaled for each GCM to a resolution of 0.05° (~5 km) for two future periods 2030–2049 (midpoint reference year = 2040) and 2080–2099 (midpoint reference year is 2090). Because climate change projections are referenced to 1990, we subtracted the temperature change between 1990 and the mean time of the measurements (2006), from climate change surfaces before applying the climate change projections. Using the previously described rate of change in temperature over the last century (0.009 °C year^{−1}) this scales to a temperature difference between 2006 and 1990 of 0.144 °C. Summary statistics describing projected future changes in air temperature and rainfall, relative to the baseline (2006), are shown in Table 2.

2.5. Analyses

All analyses were undertaken using SAS (SAS-Institute-Inc., 2000). Measurements were pooled across provenances as a two-way analysis of variance indicated that neither provenance, nor the interaction of provenance with needle age or year of sampling significantly affected CI ($P > 0.71$) or F_{ret} ($P > 0.43$).

These pooled data were used to calculate average F_{ret} and CI for all sites. F_{ret} was averaged over the two years of sampling. CI was rescaled by setting the maximum value within each of the four datasets (2 sample ages × 2 times of sampling) to 1 and expressing all values within each dataset as a fraction of this maximum. These four values were averaged to derive a single mean value for each site, referred to hereafter as CI_{norm} .

Multiple regression models describing the influence of environment on both CI_{norm} and F_{ret} were developed using the non-linear procedure (PROC NLIN) that is able to accommodate a range of linear and non-linear functional forms. Meteorological data used in the analyses included current climatic data describing average monthly and annual values for windspeed, solar radiation, total rainfall, vapour pressure deficit, and mean, minimum, maximum air temperature. Variables were introduced sequentially into the model starting with the variable that exhibited the strongest correlation, until further additions were not significant, or the mechanistic basis for influencing disease severity was not sound. Variable selection was undertaken manually, one variable at a time, and plots of residuals were examined prior to variable addition to ensure that the variable was included in the model using the least biased functional form. Model comparisons were made using the root mean square error (RMSE) and the coefficient of determination (R^2).

A range of diagnostic tests were undertaken on the developed models. Residuals were plotted against independent variables and predicted values to determine model bias. The Shapiro-Wilk test was used to determine if residuals for the final model were nor-

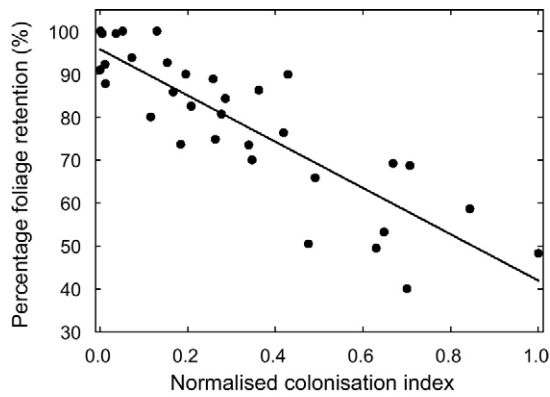


Fig. 2. Relationship between mean percentage foliage retention, F_{ret} , (averaged over both years of sampling, by site) and mean normalised colonisation index, CI_{norm} (determined as the mean of normalised colonisation index for the two needle age classes and two years of sampling, by site). The following linear line was fitted to the data: $F_{ret} = 95.80 - 53.90 CI_{norm}$ ($R^2 = 0.73$, $P < 0.001$).

mally distributed, with values over $P = 0.05$ supporting the null hypothesis that the residuals were from a normal distribution (Hatcher and Stepanski, 1994).

2.6. Model projections

Climatic variables used in the final models included mean total November rainfall and mean June air temperature. Values for these climatic variables, derived from current climate surfaces, were adjusted according to the mean monthly changes from the above described climate change projections. Spatial projections of CI_{norm} and F_{ret} were developed under current climate, while F_{ret} was projected under climate change using the 36 described scenarios to 2040 and 2090. Final graphs show projections of F_{ret} by each of the three emission scenarios, in which F_{ret} has been spatially averaged across the 12 GCMs. Regional averages of F_{ret} under both current and future climate were estimated using Regional Council administrative areas with ArcGIS. Using these data, variation in mean F_{ret} by region, between the current climate and 36 climate change scenarios were graphically displayed.

3. Results

3.1. Ranges and relationships between variables

Results for CI and F_{ret} showed a high degree of agreement between sites sampled in both 2005 and 2007. Between both years, relationships were positive and highly significant ($P < 0.001$) for CI of one-year-old foliage ($R^2 = 0.65$), CI of two-year-old foliage ($R^2 = 0.81$), and F_{ret} ($R^2 = 0.86$). When all data for both years were averaged by site, F_{ret} ranged over two-fold from 40% to 100%. Similarly, values for mean CI ranged widely from 0.01 to 24.3 for the one-year-old and 0.02 to 54.0 for the two-year-old needles (Table 1). When CI was normalised between the two age classes (CI_{norm}) to an average site value there was a strong ($R^2 = 0.73$) significant ($P < 0.001$) negative relationship between CI_{norm} and mean F_{ret} (Fig. 2).

3.2. Models and predictions of CI and foliage retention under current climate

Mean June air temperature, T_{avJune} , was positively and linearly related to CI_{norm} (Fig. 3a), with the relationship accounting for 53% of the variance in CI_{norm} . Residuals from this model showed a significant quadratic correlation with November rainfall, P_{Nov} , with

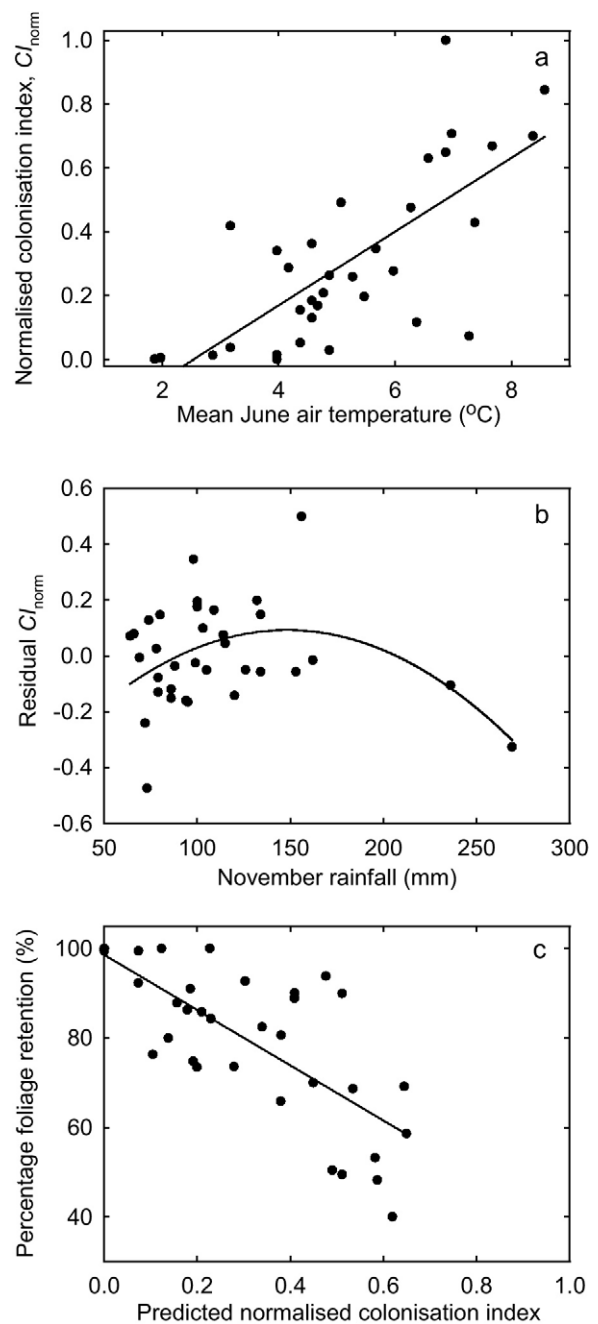


Fig. 3. Relationship between (a) mean June air temperature, T_{avJune} and mean normalised colonisation index, CI_{norm} , (b) total November rainfall, P_{Nov} , and residual CI_{norm} and (c) mean predicted CI_{norm} and percentage foliage retention, F_{ret} . Lines fitted to the data include (a) $CI_{norm} = -0.293 + 0.116T_{avJune}$ ($R^2 = 0.53$, $P < 0.001$), (b) residual $CI_{norm} = -0.503 + 8.02 \times 10^{-3}P_{Nov} - 2.71 \times 10^{-5}P_{Nov}^2$ ($R^2 = 0.19$, $P < 0.036$), and (c) $F_{ret} = 98.7 - 62.1 \text{ pred } CI_{norm}$ ($R^2 = 0.51$, $P < 0.001$).

values increasing to a predicted maximum at $149 \text{ mm month}^{-1}$, before declining at sites with higher values of P_{Nov} (Fig. 3b). Using T_{avJune} and P_{Nov} the final model for CI_{norm} was described by,

$$CI_{norm} = -0.783 + 0.112T_{avJune} + 8.12 \times 10^{-3}P_{Nov} - 2.73 \times 10^{-5}P_{Nov}^2 \quad (1)$$

with predicted values constrained to ≥ 0 . This model accounted for 65% of the variance in CI_{norm} and had a RMSE of 0.16 (Table 3). Residuals from this model were normally distributed (Shapiro-Wilk = 0.76) and exhibited little apparent bias with either predicted

Table 3
Models of best fit for predicting mean normalised colonisation index (CI_{norm}) and foliage retention (F_{ret}).

| y | Independent variables ^a | Model statistics ^b | |
|-------------|------------------------------------|-------------------------------|------|
| | | R^2 | RMSE |
| CI_{norm} | T_{avJune} | 0.53 | 0.19 |
| | T_{avJune}, P_{Nov} | 0.65 | 0.16 |
| F_{ret} | Pred CI_{norm} | 0.51 | 12.0 |

^a T_{avJune} is mean June air temperature, P_{Nov} is mean total rainfall during November.

^b The coefficient of determination (R^2) and root mean square error (RMSE) for all models are shown.

values, or independent variables (data not shown). Spatial predictions show CI_{norm} to be relatively high throughout most of the North Island, ranging from 0.1 in high altitude central North Island regions to higher than 1.0 (above max. measured values) in low altitude northern regions (Fig. 4). In contrast, most of the South Island had a substantially lower CI_{norm} due to lower T_{avJune} (Fig. 1) and the influence of the main axial ranges that results in extremely high rainfall on the west coast and relatively low rainfall on the east coast (Fig. 4).

Foliage retention exhibited a moderately strong ($R^2 = 0.51$) negative linear relationship with predicted CI_{norm} (Table 3), described by the following function,

$$F_{ret} = 98.7 - 62.1 \text{pred } CI_{norm} \quad (2)$$

with predicted values constrained between 0% and 100%. Addition of climatic variables, did not significantly improve the model. Residuals from this model were normally distributed (Shapiro-Wilk = 0.46) and exhibited little apparent bias with either predicted values, or independent variables (data not shown). Spatial variation in F_{ret} predictions largely reflect the increases in T_{avJune} that occur with decreasing latitude (south to north) or altitude within New

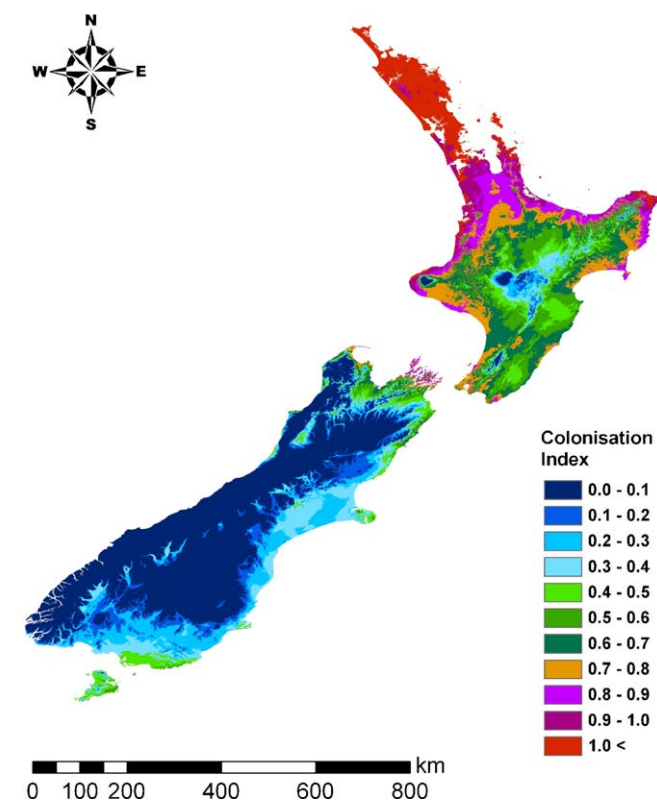


Fig. 4. Map of New Zealand showing spatial variation in mean normalised colonisation index.

Zealand (Fig. 5a). Complete foliage retention (100%) was predicted along the axial ranges of the South Island while very low values of F_{ret} (10–30%) were predicted in low altitude northern regions of the North Island (Fig. 5a).

Spatial predictions clearly highlighted the dichotomy between F_{ret} in the North and South Islands. In contrast to most of the South Island, where predicted F_{ret} was greater than 70%, the majority of the North Island had predicted F_{ret} of between 40% and 70% (Fig. 5a). Regions with greater F_{ret} in the North Island were confined to high elevation regions in central or southern regions (Fig. 5a). These predictions agreed well with the general pattern displayed by observations. South Island measurements of F_{ret} averaged 88% and ranged from 74% to 100%, while F_{ret} in the North Island averaged 65% and was less than 70% at all but four sites, three of which were located at high elevation (697–933 m) in the central North Island.

3.3. Effects of climate change on foliage retention

Projected changes in F_{ret} due to the effects of climate change on *P. gaumannii* abundance were predicted to be slight for the medium term to 2040 (Fig. 6a). Averaged across all twelve GCMs projected foliage retention at 2040 was reduced by an average of 2.8%, 3.7% and 3.7%, respectively under the B1, A1B and A2 emission scenarios (Fig. 7a). Extremes in variation in foliage retention were represented by ECHAM5 A2 and CCCma A1B which showed respective changes in F_{ret} relative to current climate of –0.30% and 5.8%, respectively (Fig. 7a).

Over the longer term, to 2090, projected reductions in foliage retention resulting from climate change, ranged from moderate to high (Fig. 6b). Compared to current climate, mean projected F_{ret} to 2090 were reduced by on average 6.5%, 10.1%, and 13.7%, under the B1, A1B and A2 emission scenarios (Fig. 7b). Reductions in foliage retention were least under CSIRO Mk3 using the B1 emission scenario (1.9%) and greatest under MIROC32 using the A2 emission scenario (16.9%) (Fig. 7b).

Regional reductions in foliage retention to 2090 showed a moderate range under the scenarios examined. With the exception of Nelson, reductions in foliage retention were considerably more marked in the North Island than South Island under all three emission scenarios (Fig. 8). Greater reductions in F_{ret} within the North Island were also evident in spatial predictions (Fig. 5). The range for foliage retention of 40–70% for the majority of land in the North Island under current climate reduces to 20–70% under climate change. Areas with predicted $F_{ret} > 70%$ were almost entirely absent within the North Island under all three climate change scenarios (Fig. 5). In the South Island F_{ret} was reduced from $>70%$ for most areas under current climate to F_{ret} of between 50% and 100%, with higher values of F_{ret} occurring in areas with high altitude. Under the most extreme A2 scenario areas with $>70%$ F_{ret} were restricted to high altitude regions along the main axial ranges (Fig. 5).

4. Discussion

Douglas-fir is the second most widely planted tree species in New Zealand production forestry after *Pinus radiata* D. Don occupying a total of 109 thousand ha or 6.1% of the total exotic plantation area (MAF, 2010). Because of its excellent wood properties Douglas-fir is widely grown for structural uses and suffers less damage on high altitude sites that experience snow than *P. radiata* (Miller and Knowles, 1994). Despite the significant volume reductions that have occurred over the last four decades following invasion of New Zealand by *P. gaumannii* (Hood and Kershaw, 1975; James and Bunn, 1978; Kimberley et al., in press) Douglas-fir remains a popular species and plantation area has more than doubled over the

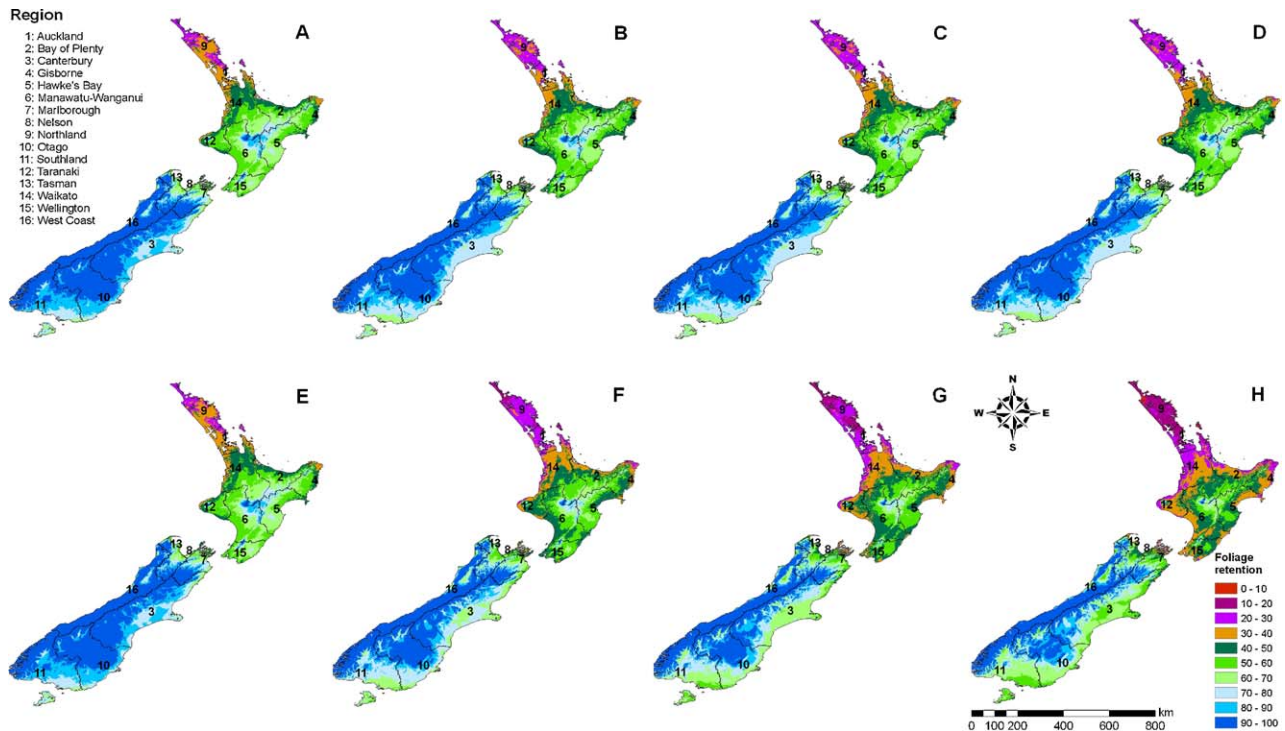


Fig. 5. Map of New Zealand showing spatial variation in predicted foliage retention under current climate (A and E) and to 2040, under the B1 (B), A1B (C) and A2 (D) emission scenarios, and to 2090 under the B1 (F), A1B (G) and A2 (H) emission scenarios.

last twenty years (Ledgard et al., 2005). Following the detection of *P. gaemannii* there was a change in practice towards earlier thinning and shorter rotation lengths in an attempt to offset disease impacts (Miller and Knowles, 1994). Growers have also established most new stands on high altitude inland sites in the southern half of the South Island where Douglas-fir generally appears healthier (Ledgard et al., 2005). As a result 76% of the current Douglas-fir resource is located in the South Island (MAF, 2010). Spatial predictions shown here under current climate reinforce grower perceptions showing disease severity to be greatest in warm, moderately wet northern areas and lowest in cooler high altitude areas in the South Island.

Colonisation index, an estimate of the relative abundance of *P. gaemannii* fruiting bodies at a particular site, was found to be strongly regulated by mean June air temperature. It is likely that air temperature has a limiting effect on the rates of colonisation of needles and fungal growth following infection (Manter et al., 2005). Functional forms reported here between these two variables were very similar to those previously found in both western Oregon and New Zealand. The similarity of climate models developed for prediction of *P. gaemannii* abundance and disease severity (i.e. F_{ret}) for New Zealand and Oregon further serves to confirm the biological and epidemiological value of these factors in explaining variation in disease severity across the landscape. CI_{norm} increased linearly from values close to 0 at a T_{avJune} of 2–3 °C, to a maximum CI_{norm} (colonisation index of approx. 24 in one-year old needles and 54 in two-year old needles) at T_{avJune} of ~8 °C, which represents the upper temperature range of all data collected. Further research should be undertaken to identify the form of the relationship above T_{avJune} of 8 °C to gain insight into how climate change will affect colonisation index in warm temperate areas, at range margins for plantation grown Douglas-fir. However, characterisation of how infection index responds to temperatures greater than 8 °C is primarily of academic interest, since little of the worldwide Douglas-fir plantation resource occurs in regions within this tem-

perature range, where faster growing pines are generally better adapted.

Our results show rainfall during late spring (November) to be an important secondary climatic determinant of infection index. Rainfall during the infection period facilitates ascospore dispersal, and free moisture on needles provides favourable conditions for spore germination and initial infection (Stone et al., 2008a). In British Columbia precipitation during the infection period has long been recognized as a factor associated with regional variation in incidence of *P. gaemannii* (Hood, 1982; McDermott and Robinson, 1989). More recent research in Oregon has shown early summer (June) leaf wetness to be a useful variable (secondary to mean winter temperature) for predicting colonisation index (Manter et al., 2005). Our results suggest that the relationship between leaf wetness and colonisation index extends across a broader rainfall range, with optimal colonisation index reached in areas with high spring rainfall (154 mm month⁻¹, or an annual rainfall in a climate with evenly distributed rainfall of 1788 mm year⁻¹). The decline in infection index at extremely high rainfall sites with ~250 mm month⁻¹ was a somewhat unexpected result and it should be noted that this decline is based on only two sites. It is possible that the high intensity rainfall that occurs in these locations may be diluting or washing off the ascospores before they are able to adhere to the needle surface. Although further research may prove this to be a spurious finding, our spatial predictions are largely insensitive to this predicted decline, as areas with these extremely high rainfalls are mainly confined to the West Coast of the South Island, where only 1% of the Douglas-fir plantation resource occurs. Similarly, this result is unlikely to be of major consequence globally because the West Coast of the South Island is unique in having the highest rainfall of the temperate, Mediterranean and continental world, across which plantation grown Douglas-fir occurs.

The strong negative relationship between foliage retention and colonisation index found here and previously (Temel et al., 2004; Hood and Kimberley, 2005; Stone et al., 2008a) has a sound theoret-

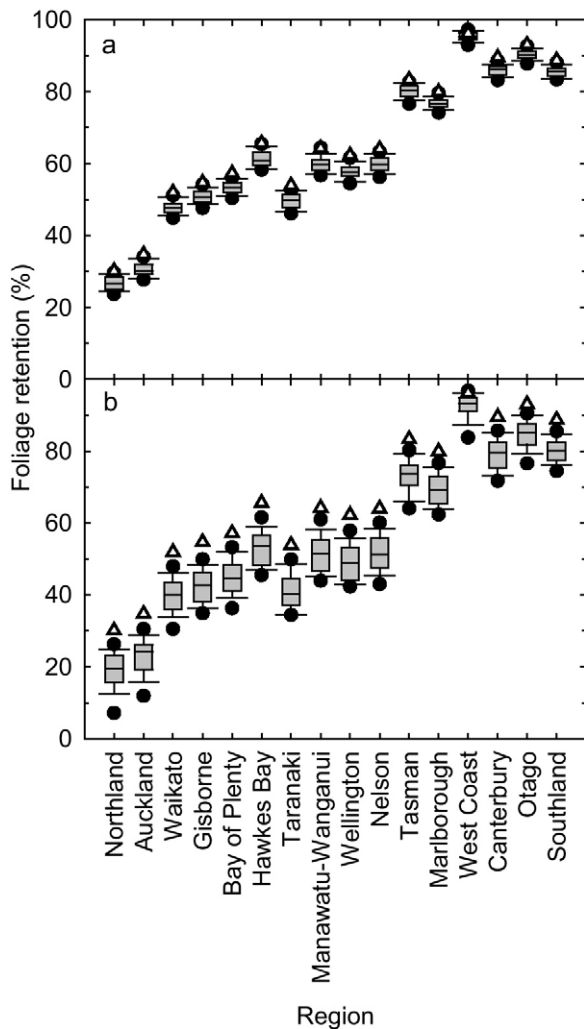


Fig. 6. Variation in mean predicted foliage retention by region (sorted in order of increasing latitude—from north to south) under current climate (triangles) and the climate change scenarios (boxplots) projected to (a) 2040 and (b) 2090. Boxplots were constructed from the 36 climate change scenarios. Boundaries of the boxplots closest to zero indicates the 25th percentile, the centre lines within the boxes indicate the median, and the boundaries of the boxes farthest from zero indicates the 75th percentile. Error bars are the tenth and 90th percentiles, and filled circles represent climate change scenarios outlying the tenth and 90th percentiles.

ical basis. Developing ascocarps of *P. gaemannii* eventually block the stomatal openings, thereby rendering the stomata nonfunctional. This impedes gas exchange and regulation of transpiration, causing impaired photosynthetic activity, and is considered the primary mechanism of pathogenicity (Manter et al., 2000; Manter et al., 2003). Estimates of the effect of *P. gaemannii* on CO₂ assimilation indicate that occlusion of about 25% of stomata results in overall negative needle carbon budgets, i.e. respiration exceeds assimilation, on an annual basis (Manter et al., 2003). Foliage abscission occurs when needles switch from being carbon sources to carbon sinks (Cannell and Morgan, 1990), usually before more than half the needle stomata are occluded, because the decrease in stomatal conductance and CO₂ fixation reduces needle carbon budgets (Manter et al., 2003). The abundance of ascocarps, i.e. higher values of colonisation index, should therefore be correlated with the principal symptom of Swiss needle cast, premature needle abscission.

Geospatial projections of future foliage retention under different climate change scenarios were found to vary widely between both the GCMs and emission scenarios. Although the B1 model is displayed for completeness, the low levels of greenhouse gas

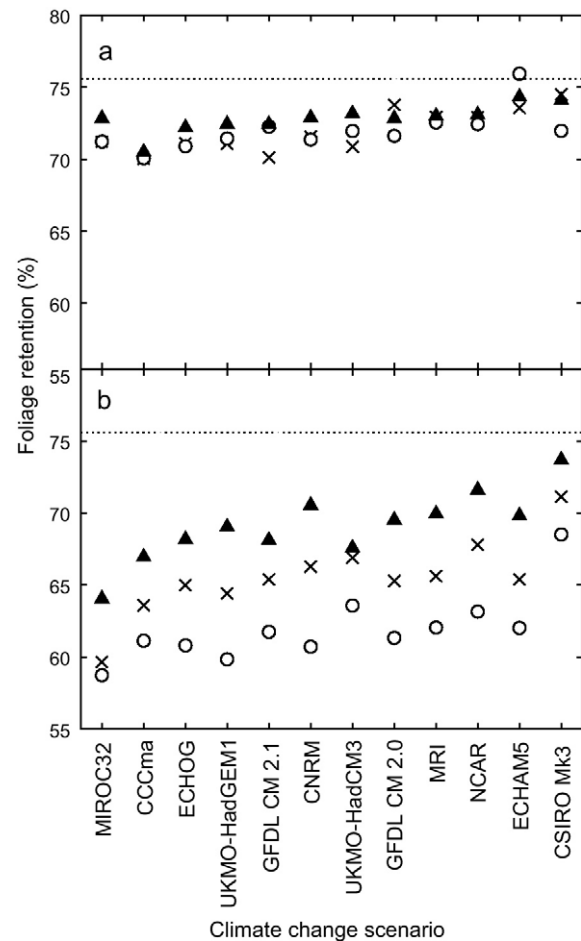


Fig. 7. Variation in mean predicted foliage retention for New Zealand under 12 models using the B1 (triangles), A1B (crosses) and A2 (open circles) emission scenarios, projected to (a) 2040 and (b) 2090. The mean predicted foliage retention under current climate is shown on both figures as a dotted line. Scenarios are sorted in descending order of mean impact of the scenario on foliage retention, averaged across both the 2040 and 2090 predictions.

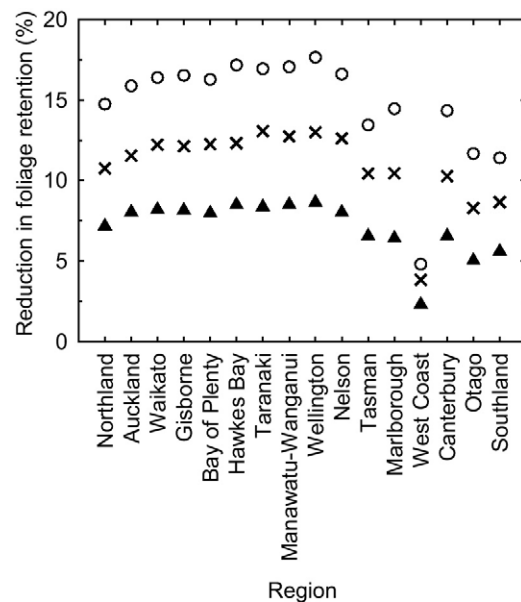


Fig. 8. Projected regional variation (sorted in order of increasing latitude—from north to south) in predicted foliage retention loss to 2090, compared to current climate, averaged across the B1 (triangles), A1B (crosses) and A2 (open circles) emission scenarios.

emissions projected under this scenario seem relatively unlikely given the current lack of political progress towards their limitation. When interpreting the results, it is also worthwhile considering the findings of Rahmstorf et al. (2007) who showed that recent trends in recorded climate change and sea level rise are effectively beyond the upper end of the emission scenarios considered by the IPCC. Therefore, the GCMs that project moderate to high temperature increases (e.g. MIROC32), and scenarios that project moderate (A1B) to high (A2) emissions should be given more weight as an indicator of future climatic conditions.

Our results suggest that climate change is likely to have the greatest impact on foliage retention and productivity of Douglas-fir over the long term in the North Island. Projections of F_{ret} to 2040 show little change from projections under current climate, as air temperature is not forecast to increase markedly within New Zealand over the medium term. However, by 2090, reductions in F_{ret} are very marked, particularly within the North Island under the A1B and A2 emission scenarios. Within the South Island, reductions in F_{ret} attributable to increasing air temperature, are dampened as the proportion of high elevation sites with air temperature below the threshold for foliage loss are greater than in the North Island. Apart from coastal and low lying regions, large areas within the South Island are projected to sustain relatively low levels of disease, and remain suitable for Douglas-fir. Climate change may also provide some opportunity to extend the species range into higher altitude South Island areas that were previously unsuitable for Douglas-fir.

Under climate change greater pathogen abundance and increased disease severity is likely to result in significant changes in plantation species composition within warmer North Island regions over the long term. Volume growth of Douglas-fir in the North Island was reduced by ca. 35% during the 15-year period after *P. gaumannii* was first detected (Kimberley et al., in press). As foliage retention is a key determinant of volume growth (Maguire et al., 2002) it is likely that there will be further losses in volume growth, particularly within coastal regions, that will approach the maximum reported losses of 50% recorded in Oregon. There is a range of suitable replacement plantation conifers available in New Zealand (e.g. *P. radiata*; *Sequoia sempervirens* (D. Don) Endl.) that match or exceed growth rates of Douglas-fir and which are not currently exposed to untreatable debilitating pests (Turner et al., 2008). Unplanned changes in species composition as a result of severe disease have already occurred in plantations in western Oregon where normally faster growing Douglas-fir has been replaced by natural regeneration of western hemlock (*Tsuga heterophylla* (Raf.) Sarg.; Hansen et al., 2000). Further research should investigate the potential impacts of climate change on long-term suitability of Douglas-fir as a plantation species in other areas where it is widely grown such as the coastal Pacific Northwest region.

Acknowledgements

This work was made possible by personnel in the following companies who facilitated access to the stands or provided information: Blakely Pacific Limited, City Forests Ltd. (Dunedin City Council), Ernslaw One Ltd., Greater Wellington Council, Hancock Forest Management NZ Ltd., Hikurangi Forest Farms Ltd., Nelson Forests Ltd., P.F. Olsen Forests, Rayonier NZ Ltd., Selwyn Plantation Board, the NZ Redwood Company, Timberlands Ltd., Winstone Pulp International, and also Gordon Baker, Margaret Conn, Aaron Morton, Peter Turner, and Morris Yeoman. We are grateful to the National Institute of Water and Atmospheric Research (NIWA) for providing the climate change scenarios and Andrew Tait for assistance in describing these scenarios in the methods. Technical, administrative or

other support was provided by: Len Coop, Judy Gardner, Sam Hendrick, Rachel Hood, the late Leith Knowles, Nick Ledgard, Charlie Low, Tod Ramsfield, Daphne Stone, and Wendy Sutton. Funding was provided by the New Zealand Foundation for Research Science and Technology (FRST CO-4X0807 Biosecurity, Protection and Risk Management of NZ Forests) the former New Zealand Douglas-fir Cooperative, and Future Forests Research. We thank an anonymous reviewer for very useful comments on a draft of the manuscript.

References

- Black, B.A., Shaw, D.C., Stone, J.K., 2010. Impacts of Swiss needle cast on overstory Douglas-fir forests of the western Oregon Coast Range. *Forest Ecology and Management* 259, 1673–1680.
- Boyce, J.S., 1940. A needle-cast of Douglas fir associated with *Adelopus gäumannii*. *Phytopathology* 40, 649–659.
- Cannell, M.G.R., Morgan, J., 1990. Theoretical study of variables affecting the export of assimilates from branches of *Picea*. *Tree Physiology* 6, 257–266.
- Hansen, E.M., Stone, J.K., Capitano, B.R., Rosso, P., Sutton, W., Winton, L., 2000. Incidence and impact of Swiss needle cast in forest plantations of Douglas-fir in coastal Oregon. *Plant Disease* 84, 773–778.
- Hatcher, L., Stepanski, E.J., 1994. A Step by Step Approach to Using the SAS System for Univariate and Multivariate Statistics. SAS Institute Inc., Cary, NC, pp. 552.
- Hood, I.A., 1982. *Phaeocryptopus gaumannii* on *Pseudotsuga menziesii* in southern British Columbia. *New Zealand Journal of Forestry Science* 12, 415–424.
- Hood, I.A., Kershaw, D.J., 1975. Distribution and infection period of *Phaeocryptopus gaumannii* in New Zealand. *New Zealand Journal of Forestry Science* 5, 201–208.
- Hood, I.A., Kimberley, M.O., 2005. Douglas fir provenance susceptibility to Swiss needle cast in New Zealand. *Australasian Plant Pathology* 34, 57–62.
- Hood, I.A., Sandberg, C.J., Barr, C.W., Holloway, W.A., Bradbury, P.M., 1990. Changes in needle retention associated with the spread and establishment of *Phaeocryptopus gaumannii* in planted Douglas fir. *European Journal of Forest Pathology*, 418–429.
- Hutchinson, M.F., Gessler, P.E., 1994. Splines—more than just a smooth interpolator. *Geoderma* 62, 45–67.
- James, R.N., Bunn, E.H., 1978. In: James, R.N., Bunn, E.H. (Eds.), A review of Douglas fir in New Zealand. FRI Symposium No. 15. Held at Rotorua, 16–19 September 1974. Forest Research Institute, New Zealand Forest Service. E.C. Keating, Government Printer, Wellington, New Zealand, pp. 455.
- Kimberley, M.O., Hood, I.A., Knowles, R.L. Impact of Swiss needle-cast on growth of Douglas-fir. *Phytopathology*, in press.
- Leathwick, J.R., Stephens, R.T.T., 1998. Climate surfaces for New Zealand. Landcare Res. Contract Report LC9798/126. Landcare Research, Lincoln, New Zealand, p. 19.
- Ledgard, N., Knowles, L., De La Mare, P., 2005. Douglas-fir – the current New Zealand scene. *New Zealand Journal of Forestry* 50, 17–21.
- MAF, 2010. A national exotic forest description as at 1 April 2009, New Zealand Ministry of Agriculture and Forestry, Wellington, New Zealand.
- Maguire, D.A., Kanaskie, A., Voelker, W., Johnson, R., Johnson, G., 2002. Growth of young Douglas-fir plantations across a gradient in Swiss needle cast severity. *Western Journal of Applied Forestry* 17, 86–95.
- Manter, D.K., Bond, B.J., Kavanagh, K.L., Rosso, P.H., Filip, G.M., 2000. Pseudothecia of the Swiss needle cast fungus, *Phaeocryptopus gaumannii*, physically block stomata of Douglas-fir, reducing CO₂ assimilation. *The New Phytologist* 148, 481–491.
- Manter, D.K., Bond, B.J., Kavanagh, K.L., Stone, J.K., Filip, G.M., 2003. Modelling the impacts of the foliar pathogen, *Phaeocryptopus gaumannii*, on Douglas-fir physiology: net canopy carbon assimilation, needle abscission and growth. *Ecological Modelling* 164, 211–226.
- Manter, D.K., Reeser, P.W., Stone, J.K., 2005. A climate-based model for predicting geographic variation in Swiss needle cast severity in the Oregon Coast Range. *Phytopathology* 95, 1256–1265.
- Marks, G.C., Smith, I.W., Cook, I.O., 1989. Spread of *Dothistroma septospora* in plantations of *Pinus radiata* in Victoria between 1979 and 1988. *Australian Forestry*, 52.
- McDermott, J.M., Robinson, R.A., 1989. Provenance variation for disease resistance in *Pseudotsuga menziesii* to the Swiss needle cast pathogen, *Phaeocryptopus gaumannii*. *Canadian Journal of Forest Research* 19, 244–246.
- Miller, J.T., Knowles, F.B., 1994. Introduced forest trees in New Zealand. Recognition, role and seed source. 14. Douglas-fir, *Pseudotsuga menziesii* (Mirbel) Franco. FRO Bulletin No. 124. New Zealand Forest Research Institute Limited, Rotorua, New Zealand. 38 pp.
- Ministry for the Environment, 2008. Climate change effects and impacts assessment. A guidance manual for local government in New Zealand. 2nd ed. Prepared for the Climate Change Office by Mullan, B., Wratt, D., Dean, S., Hollis, M., Allan, S., Williams, T., Kenny, G., MfE Publication ME 870, p. 149. <http://www.mfe.govt.nz/publications/climate/climate-change-effect-impacts-assessments-may08/climate-change-effect-impacts-assessment-may08.pdf> (accessed April 2010).
- Morton, H.L., Patton, R.F., 1970. Swiss needle-cast of Douglas fir in the Lake States. *Plant Disease Reporter* 54, 612–616.
- New Zealand Meteorological Service, 1983. Summaries of Climatological Observations to 1980. NZ Met. Serv. Misc. Pub., no. 177, p. 172.

- NIWA, 2010. New Zealand temperature record. Available at <http://www.niwa.co.nz/our-science/climate/news/all/nz-temp-record> (last accessed on 25 June, 2010).
- Peace, T.R., 1962. Pathology of Trees and Shrubs with Special Reference to Britain. Clarendon Press, p. 753.
- Rahmstorf, S., Cazenave, A., Church, J.A., Hansen, J.E., Keeling, R.F., Parker, D.E., Somerville, R.C.J., 2007. Recent climate observations compared to projections. *Science* 316, 709.
- Salinger, M.J., 1981. New Zealand Climate: The instrumental record. Thesis submitted for the degree of Doctor of Philosophy at the Victoria University of Wellington, January 1981.
- SAS-Institute-Inc., 2000. SAS/STAT User's Guide: Version 8. Volumes 1, 2 and 3. SAS Institute Inc., Cary, North Carolina, pp. 3884.
- Stone, J.K., Capitano, B.R., Kerrigan, J.L., 2008a. The histopathology of *Phaeocryptopus gaeumannii* on Douglas-fir needles. *Mycologia* 100, 431–444.
- Stone, J.K., Coop, L.B., Manter, D.K., 2008b. Predicting effects of climate change on Swiss needle cast disease severity in Pacific Northwest forests. *Canadian Journal of Plant Pathology-Revue Canadienne de Phytopathologie* 30, 169–176.
- Stone, J.K., Hood, I.A., Watt, M.S., Kerrigan, J.L., 2007. Distribution of Swiss needle cast in New Zealand in relation to winter temperature. *Australasian Plant Pathology* 36, 445–454.
- Temel, F., Johnson, G.R., Stone, J.K., 2004. The relationship between Swiss needle cast symptom severity and level of *Phaeocryptopus gaeumannii* colonization in coastal Douglas-fir (*Pseudotsuga menziesii* var. *menziesii*). *Forest Pathology* 34, 383–394.
- Temel, F., Stone, J.K., Johnson, G.R., 2003. First report of Swiss needle cast caused by *Phaeocryptopus gaeumannii* on Douglas-fir in Turkey. *Plant Disease* 87, 1536.
- Turner, J.A., West, G., Dungey, H., Wakelin, S., Maclaren, P., Adams, T., Silcock, P., 2008. Managing New Zealand planted forests for carbon: A review of selected management scenarios and identification of knowledge gaps. MAF report No. CC MAF POL.2008–09 (108-1).